

Stress relaxation behavior of prestressing strands under low temperatures

Jia-Bao Yan, Jian Xie, and Kanran Ding

- Through a test program of 18 specimens, this paper documents a study of the stress relaxation behavior of steel strand under a combination of prestressing levels and low temperatures.
- As a result of the test program, a mathematical model was developed to describe the relationship between stress relaxation of the steel strands and various prestressing levels and low temperatures.
- Design recommendations were made for predicting stress relaxation behavior based on the model and test program.

PCI Journal (ISSN 0887-9672) V. 65, No. 1, January–February 2020.

PCI Journal is published bimonthly by the Precast/Prestressed Concrete Institute, 200 W. Adams St., Suite 2100, Chicago, IL 60606.

Copyright © 2020, Precast/Prestressed Concrete Institute. The Precast/Prestressed Concrete Institute is not responsible for statements made by authors of papers in *PCI Journal*. Original manuscripts and discussion on published papers are accepted on review in accordance with the Precast/Prestressed Concrete Institute's peer-review process. No payment is offered.

Precast, prestressed concrete and prestressed steel structures have been used in many applications, such as bridges, buildings, and nuclear cooling towers. More recently, precast, prestressed concrete offshore platforms have offered solutions for the exploration of oil and gas in the Arctic region, which holds about 13% of the undiscovered oil and 30% of the undiscovered gas in the world.^{1–3} Precast, prestressed concrete structures in the Arctic region are challenged by the harsh environment, especially the low temperatures, which reach about -70°C (-94°F).⁴

Due to the rapid economic development of the People's Republic of China, precast, prestressed concrete structures—for example, railway bridges and facility buildings, large-span factories, and bridges—are more common in Tibet and northern China. These precast, prestressed concrete structures are also exposed to temperatures below -50°C (-58°F).^{5–6}

Another example of a precast, prestressed concrete structures used in low temperatures is containers for liquified natural gas. If there were leakage, the precast, prestressed concrete wall would be exposed to extremely low temperatures of about -165°C (-265°F).⁶ These precast, prestressed concrete structures may be subjected to low or extremely low temperatures throughout their service lives. Therefore, the evaluation of the performances of these structures needs to consider the effects of such temperatures to ensure safe performance.

The mechanical properties of steel reinforcement or concrete at low or extremely low temperatures have been extensively studied. Elices et al.⁶ and Lahlou et al.⁷ conducted pilot research on the strength behavior of steel reinforcement and concrete at cryogenic temperatures. Ehlers and Østby⁸ investigated the effects of low temperatures on the impact resistance of steel ship hulls. Yan et al.³ presented experimental studies on the mechanical properties of mild steel and high-strength steel at low Arctic temperatures. These studies focused on the material level (mainly on the reinforcement and concrete) of the reinforced concrete structures at low temperatures.

Planas et al.⁹ presented the mechanical properties of steel strand at -165°C (-265°F). Nie¹⁰ experimentally studied the mechanical properties of steel strand at low temperatures from -165°C to 20°C (68°F). Liu et al.¹¹ and Chen and Liu¹² investigated the thermal expansive behavior of steel strand used in large-span spacing structures. Based on these reported test results, most of the previous studies focused on the mechanical properties of the steel reinforcement, steel strand, or concrete at low temperatures.

Few studies have focused on the stress relaxation of steel strand at different low temperatures. Moreover, the losses of tension by relaxation of steel strand after prestressing were neglected in previous studies.¹³ Therefore, it is of interest to investigate stress relaxation of steel strand after prestressing at different low temperatures to evaluate the prestressing levels. These results will contribute to the design of precast, prestressed concrete structures at different low temperatures.

A test program consisting of 18 seven-wire strand specimens was conducted to investigate the stress relaxation of

steel strand under different combinations of prestressing stress and low temperatures. Three prestressing levels and four temperature levels were chosen. The specimens are identified with a letter and two numbers. The letter represents the temperature. A is -20°C, B is -40°C, C is -100°C, and D is -165°C. The number directly following the letter represents the initial prestressing ratio, with 1 being 0.75, 2 being 0.65, and 3 being 0.5. The letter following the hyphen is the identification number for two identical specimens. A special testing rig with a cooling chamber was designed to simulate the low-temperature environment to -165°C (-265°F). Liquid nitrogen was used to cool the specimens for testing. Prestressing rigs were also used for the prestress application.

The effects of the low temperature and prestressing levels on the stress relaxation are presented and discussed. Based on the test results, regression analysis was carried out to develop mathematical models to describe the relationship between stress relaxation and the temperature and prestressing force. Finally, based on these experimental and analytical studies, design recommendations are given for the prediction of the stress relaxation of steel strand for a combination of low temperatures and prestressing forces.

Stress relaxation of steel strand at low temperatures and under prestressing forces

Specimens

This test program used seven-wire steel strand with a diameter of 15.2 mm (0.6 in.) (Fig. 1), which is widely used in precast, prestressed concrete structures. The elastic modulus, yield strength, and fracture strain of the steel strand were 198 GPa (28,717 ksi), 1860 MPa (270 ksi), and 0.05, respectively. The ultimate force obtained from the tensile test was 264.18 kN (59.39 kip) for this type of steel strand.

Eighteen steel strands measuring 3 m (9.84 ft) in length were prepared in this test program. Each specimen only included strand and was not encased in concrete. The key parameters for the test program were temperature and prestressing force applied on the strands. Four temperatures levels, 20°C, -40°C, -100°C, and -165°C (68°F, -40°F, -148°F, and -265°F), were selected, and specimens were categorized into four groups, A to D, by their applied temperature level. Three prestressing levels were designed for specimens in groups A and B, and two prestressing levels were designed for specimens in groups C and D. Considering the initial prestressing force and limits according to the Chinese standard GB 50010-2010,¹⁴ the prestress levels of $0.5F_u$, $0.65F_u$, and $0.75F_u$ were applied to the specimens in each group at different low temperatures, where F_u is the ultimate tensile resistance of the steel strand. The 18 specimens consisted of two identical specimens prepared for each prestressing level at a given temperature level. Table 1 gives the details of the specimens.

Table 1. Details of the specimens

Specimen	Temperature range, °C	Initial prestressing ratio, F_t/F_u
A1-1, A1-2	20	0.75
A2-1, A2-2	20	0.65
A3-1, A3-2	20	0.5
B1-1, B1-2	-40	0.75
B2-1, B2-2	-40	0.65
C1-1, C1-2	-100	0.75
C2-1, C2-2	-100	0.65
D1-1, D1-2	-165	0.75
D2-1, D2-2	-165	0.65

Note: There were two specimens for each temperature and initial prestressing ratio combination. F_t = prestressing force applied to steel strand; F_u = ultimate tensile resistance of steel strand. °F = (°C × 1.8) + 32.

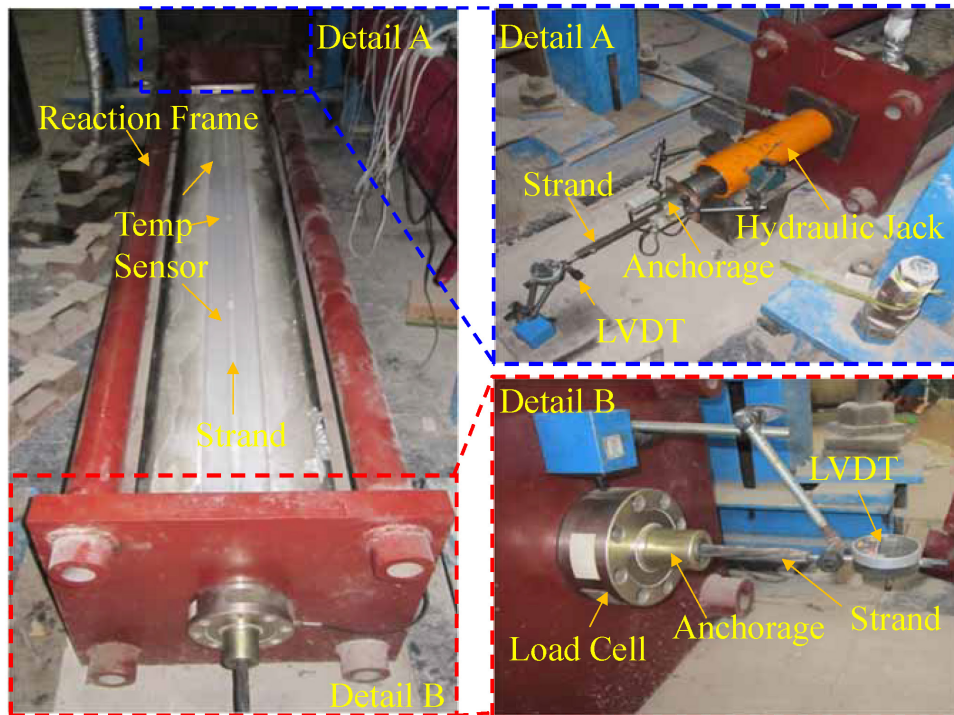
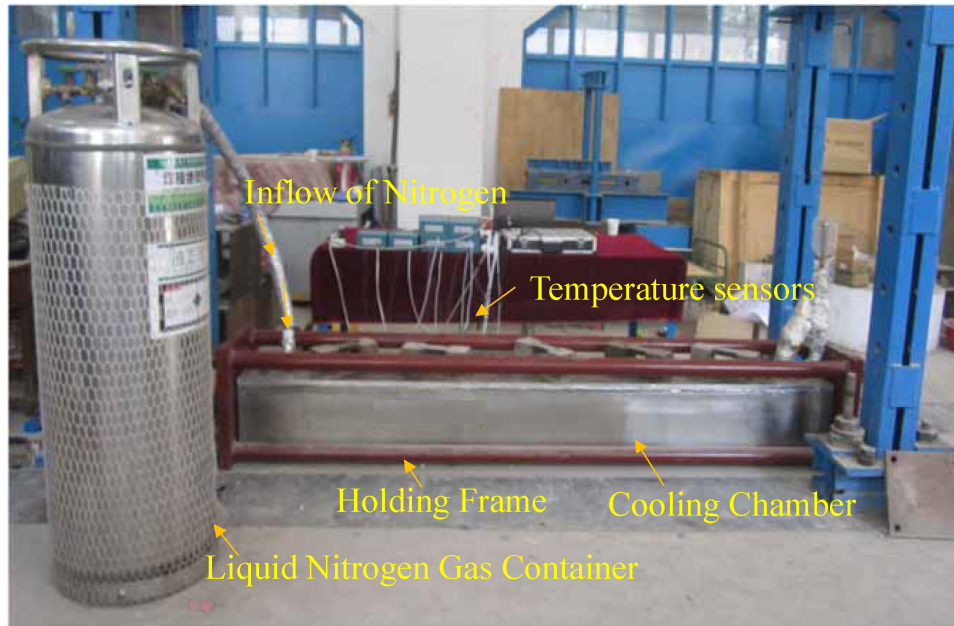
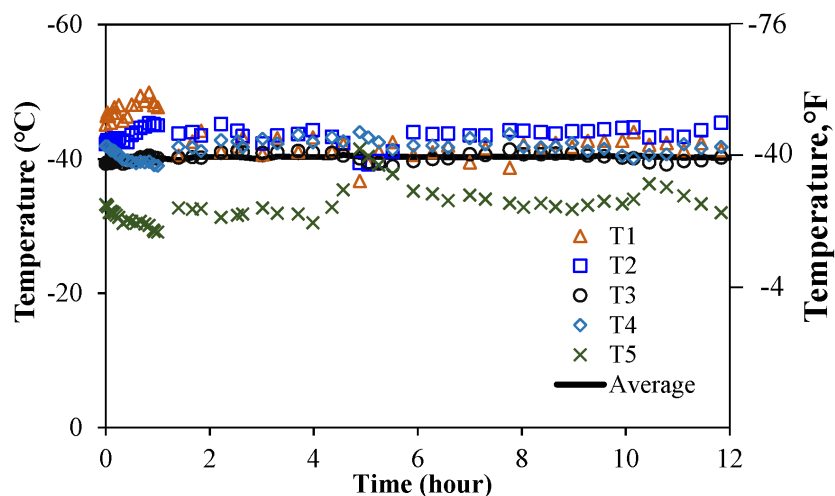


Figure 1. Test setup. Note: LVDT = linear variable displacement transducer.

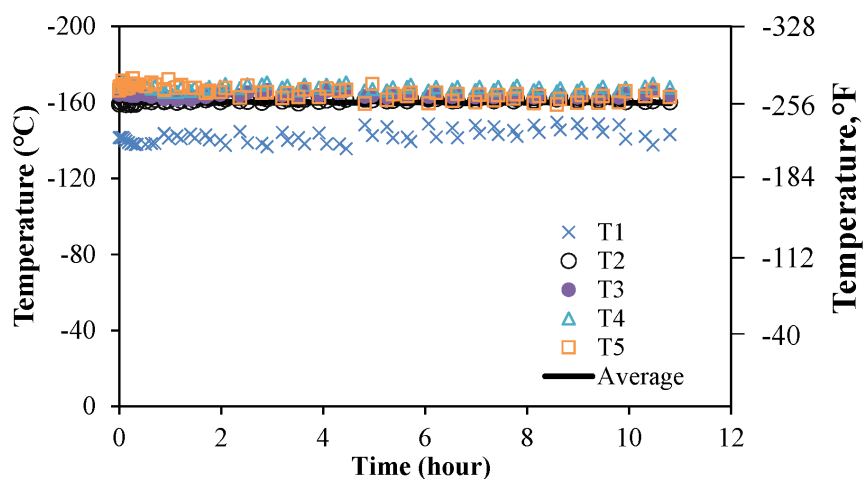
Test setup and measurements

In the test, all of the specimens were subjected to the assigned prestressing force and low temperature. To achieve this objective, a rigid testing frame with a cooling chamber was fabricated (Fig. 1). The rigid reaction frame was designed to apply the prestressing force on the steel strands.

The cooling chamber with insulation materials used liquid nitrogen to simulate the low-temperature environment. The liquid nitrogen was injected into the cooling system with steel pipes and a tubular radiator that circles inside the chamber. Thus, the lowest temperature for testing at -165°C (-265°F) was achieved. Five PT100-type thermal sensors were evenly distributed on the steel strands at different



Specimen B2-2



Specimen D1-2

Figure 2. Temperature history for specimens B2-2 and D1-2. Note: T1 = sensor 1; T2 = sensor 2; T3 = sensor 3; T4 = sensor 4; T5 = sensor 5.

locations to monitor the temperature distribution inside the chamber. A hydraulic jack was used to apply the prestressing force on the steel strands. A steel frame was designed with four steel columns; the total cross-sectional area of these four columns was 19,804 mm² (30.7 in.²), or 140 times that of the steel strands. This much higher stiffness of the frame was to minimize the error of the stress relaxation of the steel strands due to deformation of the reaction frame.

The steel strands were first put inside the cooling chamber with the two ends attached to the reaction frame with the anchorage. A load cell (Fig. 1) was installed outside the cooling chamber that connects the anchorage and rigid frame, which was used to record the reaction force acting on the strands. Thermal sensors were then installed on the steel strands to monitor their temperature. Liquid nitrogen was then injected into the chamber to cool the steel strands

to the target temperature. According to the Chinese standard GB/T 10120-2013,¹⁵ stress relaxation tests must be carried out after one hour of cooling the steel strands to the target temperature. Prestressing of the strands to the target tension force F_0 was carried out in three stages. In the first stage, a force of $0.2F_0$ was applied to the steel strands. In the second stage, the steel strands were prestressed from $0.2F_0$ to $1.0F_0$ in four steps of two minutes each. Finally, it took about two minutes to maintain the strands at the target prestressing force F_0 and the timer was set to zero; this time point is denoted as t_0 . Two linear variable displacement transducers were installed on the ends of the steel strands to monitor their elongation or shortening (Fig. 1). The strain and temperature of the strands were recorded at different times. The temperature was maintained by controlling the flow velocity of the liquid nitrogen into the cooling chamber with the temperature control valve (Fig. 1).

Figure 2 shows the temperatures measured by the five sensors over time. The cooling system achieved the average target temperatures to guarantee the accuracy of the tests on stress relaxation of steel strand at low temperatures.

Duration of steel-strand stress relaxation tests at low temperatures

According to the Chinese standard GB/T 21839-2008,¹⁶ 100 hours are required for the stress relaxation of steel strand under prestressing at ambient temperature. However, 100 hours for each stress relaxation test at low temperatures would be costly and time-consuming. Therefore, in this test program, only six specimens in group A and specimen B1-1 were tested for 100 hours, and the other specimens were tested for 12 hours. Based on the test data for 12 hours, the authors developed mathematical models to predict stress relaxation behavior at times less than 100 hours and modify the data for the tests conducted for less than 100 hours. These predictions contributed to the mathematical models to predict the stress relaxation of the steel strands at different low temperatures.

Test results and discussions

Modifications to steel-strand stress relaxation test data

During the tests on the stress relaxation of the steel strands, thermal expansion caused by temperature changes affected the stress of the steel strands. For example, change of the temperature ΔT resulted in the change in stress $\Delta\sigma$ given in Eq. (1).

$$\Delta\sigma = \Delta\varepsilon E_s = (\alpha_t \Delta T) E_s \quad (1)$$

where

E_s = Young's modulus of elasticity of steel strand

α_t = linear expansion of steel strand

For the steel strand used in this study with a yield strength of 1860 MPa (270 ksi), a change in temperature of 1°C (1.8°F) produces about 2 MPa (0.3 ksi) of thermal expansion stress, which is about 10% of the stress relaxation of the steel strand after 100 hours of prestressing. Therefore, the test data obtained from the stress relaxation test need to consider these thermal expansion strains in the steel strand and testing frame.

Figure 3 shows the geometric details of the steel strand and test setup. Because the temperature varies along the whole length of the steel strand, the force produced by the thermal expansion mainly includes the force produced by thermal expansion of the strand inside the chamber (length equals l_3 , as shown in Fig. 3), thermal expansion of the strand on the left and right sides of the cooling chamber (length equals l_1 or l_2 , as shown in Fig. 3), and thermal expansion by the frame.

The force produced by the thermal expansion of the strand inside the chamber (length equals l_3 , as shown in Fig. 3) can be determined with Eq. (2).

$$\Delta F_1 = \alpha_m (T_n - T_0) E_s \left(\frac{l_3}{l} \right) A_{ps} \quad (2)$$

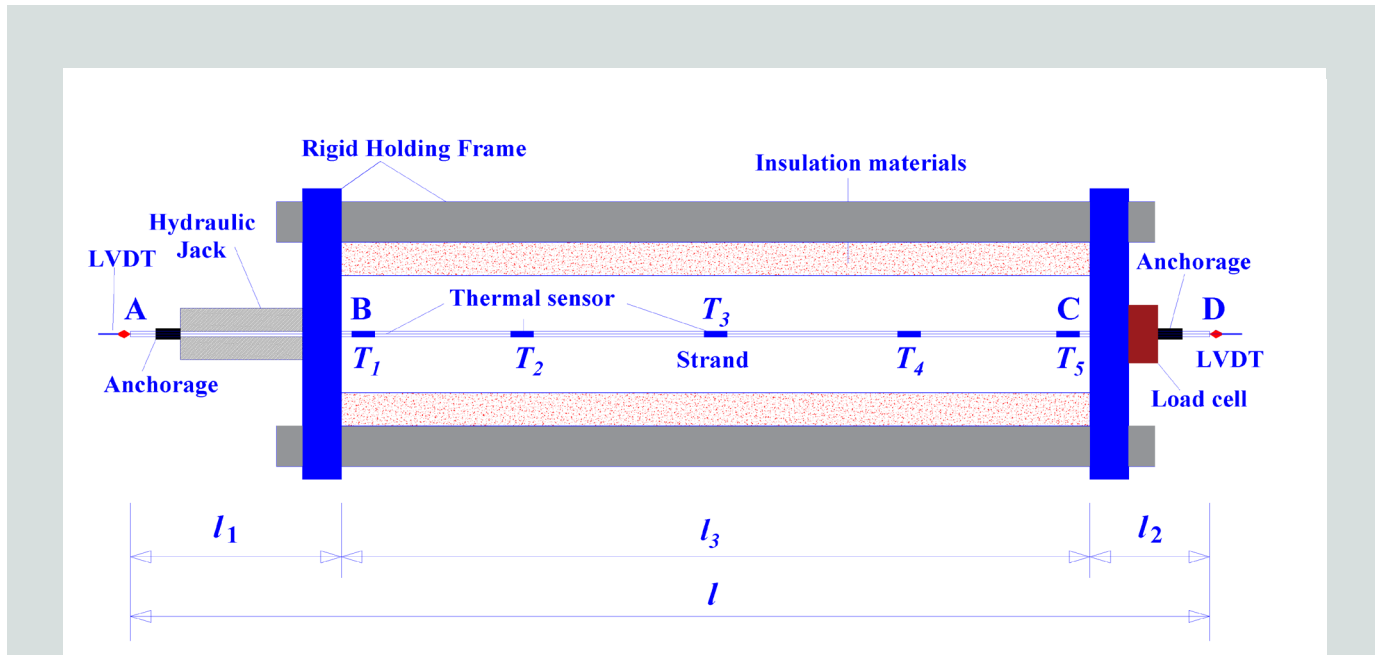


Figure 3. Schematic of test setup. Note: A = location A; B = location B; C = location C; D = location D; l = total length of steel strand; l_1 = length of steel strand outside cooling chamber; l_2 = length of steel strand outside cooling chamber; l_3 = length of steel strand in cooling chamber; LVDT = linear variable displacement transducer.

where

ΔF_1 = modified prestressing force acting on the steel strand due to linear expansion of strand inside the cooling chamber

T_n = testing temperature in the chamber at current time t_n

T_0 = testing temperature in the chamber at time t_0

α_m = linear expansion coefficient at temperature $(T_n + T_0)/2$

l_3 = length of steel strand in the cooling chamber

l = total length of steel strand

A_{ps} = cross-sectional area of steel strand

The force produced by the thermal expansion of the strand outside the chamber (length equaling l_1 or l_2 , as shown in Fig. 3) can be determined with Eq. (3) and (4).

$$\Delta F_{o,l} = \alpha_{m,l} (T_{n,l} - T_{0,l}) E_s \left(\frac{l_1}{l} \right) A_{ps} \quad (3)$$

$$\Delta F_{o,r} = \alpha_{m,r} (T_{n,r} - T_{0,r}) E_s \left(\frac{l_2}{l} \right) A_{ps} \quad (4)$$

where

$\Delta F_{o,l}$ = modified prestressing force acting on the steel strand outside the chamber along l_1 (Fig. 3)

$\Delta F_{o,r}$ = modified prestressing force acting on the steel strand outside the chamber along l_2 (Fig. 3)

$T_{n,l}$ = average value of the temperature at location A in Fig. 3 and ambient temperature at current time t_n

$T_{n,r}$ = average value of the temperature at location B in Fig. 3 and ambient temperature at current time t_n

$T_{0,l}$ = average value of the temperature at the location A in Fig. 3 and ambient temperature at time t_0

$T_{0,r}$ = average value of the temperature at the location B in Fig. 3 and ambient temperature at time t_0

$\alpha_{m,l}$ = linear expansion coefficient corresponding to $(T_{n,l} + T_{0,l})/2$

$\alpha_{m,r}$ = linear expansion coefficient corresponding to $(T_{n,r} + T_{0,r})/2$

l_1, l_2 = length of steel strand outside cooling chamber (Fig. 3)

The force produced by the thermal expansion of the holding

frame for the test rig (Fig. 3) can be determined using Eq. (5).

$$\Delta F_F = \alpha_{t,f} (T_n - T_0) E_s \left(\frac{l_3}{l} \right) A_{ps} \quad (5)$$

where

$\alpha_{t,f}$ = linear expansion coefficient of the holding frame

l_3 = length between the holding frame (Fig. 3)

Moreover, the error force due to the strain deformation of the strand itself can be determined with Eq. (6).

$$\Delta F_D = (X_n - X_0) \frac{E_s A_{ps}}{l_3} \quad (6)$$

where

X_n = relative displacement of the strand monitored by the two linear variable displacement transducers installed on the two ends of the strand at time t_n

X_0 = relative displacement of the strand monitored by the two linear variable displacement transducers installed on the two ends of the strand at time t_0

l_3 = length between the holding frame

These forces need to be considered to calculate the true prestressing force that is actually applied to the steel strand.

Stress relaxation behavior

General behavior Steel strand prestressed at two end points will partially lose its prestress due to creep. The relaxation rate of the prestress R describes the degree of prestress loss, which is defined by Eq. (7).

$$R = \frac{(\sigma_{s0} - \sigma_{st})}{\sigma_{s0}} \quad (7)$$

where

σ_{s0} = prestress at initial state

σ_{st} = prestress at time t

Tables 2 to 5 gives the average relaxation rates of the steel strands subjected to different prestressing levels and low temperatures. **Figure 4** shows the representative prestress and relaxation rate curves, respectively, of the steel strands at ambient temperature over time. **Figure 5** shows the representative prestress and relaxation rate curves, respectively, of the steel strands at a low temperature over time. These curves show that as the time t increased, the prestress of the steel strands decreased at both ambient and low temperatures. The steel strands exhibit the highest relaxation rate during the first five hours after prestressing. Between 5 and 20 hours after prestressing, the relaxation rate of the steel strands slows. After 20 hours, the steel-strand relaxation rate

Table 2. Tests and predicted relaxation rate ratios for steel strands at 20°C and prestressing stress

Specimen	P_r	t , hours	R , %	R_p , %	R/R_p
A1	0.75	0.3	0.32	0.45	0.70
	0.75	0.5	0.42	0.51	0.83
	0.75	1.0	0.53	0.57	0.94
	0.75	2.0	0.58	0.63	0.92
	0.75	5.0	0.71	0.73	0.97
	0.75	8.0	0.73	0.79	0.92
	0.75	10.0	0.74	0.82	0.90
	0.75	15.0	0.85	0.87	0.97
	0.75	20.0	0.92	0.91	1.01
	0.75	30.0	0.98	0.98	1.01
	0.75	40.0	1.00	1.02	0.98
	0.75	50.0	1.13	1.06	1.07
	0.75	60.0	1.20	1.09	1.10
	0.75	70.0	1.37	1.12	1.22
	0.75	100.0	1.34	1.18	1.13
A2	0.65	0.3	0.21	0.34	0.60
	0.65	0.5	0.29	0.38	0.76
	0.65	1.0	0.37	0.43	0.87
	0.65	2.0	0.44	0.48	0.93
	0.65	5.0	0.61	0.55	1.11
	0.65	8.0	0.66	0.59	1.10
	0.65	10.0	0.70	0.62	1.14
	0.65	15.0	0.77	0.66	1.17
	0.65	20.0	0.80	0.69	1.16
	0.65	30.0	0.90	0.73	1.23
	0.65	40.0	0.97	0.77	1.26
	0.65	50.0	1.05	0.80	1.33
	0.65	60.0	0.99	0.82	1.21
	0.65	70.0	1.10	0.84	1.31
	0.65	100.0	1.23	0.89	1.38
A3	0.5	0.3	0.17	0.20	0.86
	0.5	0.5	0.26	0.23	1.17
	0.5	1.0	0.30	0.25	1.20
	0.5	2.0	0.39	0.28	1.38
	0.5	5.0	0.41	0.33	1.27
	0.5	8.0	0.37	0.35	1.05
	0.5	10.0	0.39	0.36	1.07
	0.5	15.0	0.41	0.39	1.06
	0.5	20.0	0.45	0.41	1.12
	0.5	30.0	0.47	0.43	1.09
	0.5	40.0	0.40	0.45	0.89
	0.5	50.0	0.57	0.47	1.21
	0.5	60.0	0.48	0.48	0.99
	0.5	70.0	0.57	0.50	1.15
	0.5	100.0	0.66	0.53	1.25

Note: For all temperatures, the mean was 1.02 and the coefficient of variation was 0.21. P_r = prestressing level; R = relaxation rate of the prestress; R_p = predicted relaxation rate; t = time. °F = (°C × 1.8) + 32.

Table 3. Tests and predicted relaxation rate ratios for steel strands at -40°C and prestressing stress

Specimen	P_r	t , hours	R , %	R_p , %	R/R_p
B1	0.75	0.3	0.47	0.44	1.05
	0.75	0.5	0.43	0.50	0.85
	0.75	1.0	0.44	0.55	0.80
	0.75	2.4	0.46	0.64	0.72
	0.75	4.9	0.54	0.71	0.76
	0.75	8.0	0.53	0.77	0.69
	0.75	20.0	0.71	0.89	0.79
	0.75	29.0	0.70	0.95	0.74
	0.75	40.0	0.67	1.00	0.67
	0.75	50.0	0.72	1.03	0.69
	0.75	66.0	0.78	1.08	0.73
	0.75	71.0	0.84	1.09	0.77
	0.75	80.0	0.87	1.12	0.78
	0.75	89.0	0.78	1.13	0.68
	0.75	98.9	0.95	1.15	0.83
B2	0.65	0.3	0.32	0.33	0.95
	0.65	0.5	0.35	0.37	0.95
	0.65	1.1	0.42	0.42	0.99
	0.65	2.0	0.44	0.46	0.96
	0.65	3.1	0.46	0.50	0.92
	0.65	4.1	0.49	0.52	0.94
	0.65	5.0	0.49	0.54	0.92
	0.65	6.8	0.52	0.56	0.92
	0.65	7.9	0.53	0.58	0.92
	0.65	10.1	0.57	0.60	0.95
	0.65	10.7	0.54	0.61	0.89
	0.65	11.6	0.57	0.62	0.93
	0.65	12.0	0.56	0.62	0.91
	0.65	13.5	0.63	0.63	1.00
	0.65	14.4	0.64	0.64	1.00

Note: For all temperatures, the mean was 1.02 and the coefficient of variation was 0.21. P_r = prestressing level; R = relaxation rate of the prestress; R_p = predicted relaxation rate; t = time. °F = (°C × 1.8) + 32

slows and becomes stable. For example, for a steel strand at a low temperature of -40°C (-40°F), the relaxation rates at 5, 20, and 100 hours after prestressing are about 0.5%, 0.7%, and 0.8%, respectively.

Effect of time on steel-strand relaxation The relaxation rate of the steel strands increased as the time t increased (Fig. 6). The relaxation rate increased sharply after prestressing the steel strand and then slowed down. This paper uses the velocity of the relaxation rate V_R to describe the change in relaxation rate according to Eq. (8).

$$V_R = \frac{(R_{t2} - R_{t1})}{t_2 - t_1} \quad (8)$$

Table 4. Tests and predicted relaxation rate ratios for steel strands at -165°C and prestressing stress

Specimen	P_r	t , hours	R , %	R_p , %	R/R_p
C1	0.75	0.2	0.51	0.42	1.21
	0.75	0.5	0.66	0.47	1.40
	0.75	1.0	0.77	0.54	1.43
	0.75	2.2	0.84	0.61	1.38
	0.75	3.1	0.85	0.64	1.32
	0.75	4.0	0.85	0.67	1.26
	0.75	5.1	0.84	0.70	1.21
	0.75	6.2	0.87	0.72	1.22
	0.75	7.1	0.90	0.73	1.22
	0.75	9.5	0.94	0.77	1.22
	0.75	10.5	0.96	0.78	1.23
	0.75	11.7	0.98	0.80	1.23
	0.75	12.0	0.99	0.80	1.24
	0.75	12.5	0.88	0.80	1.09
	0.75	13.0	0.89	0.81	1.10
C2	0.65	0.3	0.34	0.34	1.00
	0.65	0.7	0.41	0.38	1.09
	0.65	1.0	0.46	0.41	1.14
	0.65	2.1	0.49	0.45	1.08
	0.65	3.1	0.54	0.48	1.11
	0.65	4.2	0.55	0.51	1.08
	0.65	5.1	0.54	0.52	1.03
	0.65	6.0	0.55	0.54	1.03
	0.65	7.0	0.57	0.55	1.03
	0.65	8.5	0.59	0.57	1.04
	0.65	10.1	0.59	0.58	1.02
	0.65	11.4	0.59	0.59	1.00
	0.65	12.1	0.59	0.60	0.98
	0.65	12.8	0.59	0.61	0.97
	0.65	13.2	0.61	0.61	0.99

Note: For all temperatures, the mean was 1.02 and the coefficient of variation was 0.21. P_r = prestressing level; R = relaxation rate of the prestress; R_p = predicted relaxation rate; t = time. °F = (°C × 1.8) + 32.

Table 5. Tests and predicted relaxation rate ratios for steel strands at -100°C and prestressing stress

Specimen	P_r	t , hours	R , %	R_p , %	R/R_p
D1	0.75	0.5	0.64	0.46	1.40
	0.75	1.0	0.74	0.51	1.44
	0.75	2.1	0.79	0.57	1.37
	0.75	2.9	0.85	0.61	1.39
	0.75	4.1	0.82	0.64	1.28
	0.75	4.9	0.81	0.66	1.23
	0.75	6.3	0.89	0.69	1.30
	0.75	7.0	0.88	0.70	1.26
	0.75	8.2	0.90	0.72	1.26
	0.75	8.6	0.88	0.72	1.22
	0.75	9.0	0.81	0.73	1.12
	0.75	9.5	0.89	0.73	1.22
	0.75	10.0	0.88	0.74	1.19
	0.75	10.5	0.95	0.74	1.28
	0.75	12.0	0.94	0.76	1.23
D2	0.65	1.1	0.43	0.39	1.09
	0.65	2.1	0.37	0.43	0.85
	0.65	3.1	0.30	0.46	0.65
	0.65	4.6	0.33	0.49	0.68
	0.65	5.3	0.37	0.50	0.74
	0.65	7.0	0.33	0.52	0.63
	0.65	8.1	0.39	0.54	0.73
	0.65	9.0	0.33	0.55	0.60
	0.65	10.2	0.38	0.56	0.68
	0.65	10.6	0.36	0.56	0.64
	0.65	11.1	0.37	0.56	0.66
	0.65	11.6	0.45	0.57	0.80
	0.65	12.1	0.33	0.57	0.58

Note: For all temperatures, the mean was 1.02 and the coefficient of variation was 0.21. P_r = prestressing level; R = relaxation rate of the prestress; R_p = predicted relaxation rate; t = time. °F = (°C × 1.8) + 32.

where

R_{t_2} = relaxation rate at time t_2

R_{t_1} = relaxation rate at time t_1

Figure 7 shows the velocity of the relaxation rate over time for the steel strands at different low temperatures. During approximately the first half hour, the steel strands exhibited the highest relaxation rate velocity. After about one hour, the VR ratio became stable. For example, the V_R ratio for specimen A3-1 at $t = 0.25$ hours was 0.7%/hour, and it decreased to 0.35%/hour at $t = 0.5$ hours after prestressing. After five hours of prestressing, V_R decreased to 0.008%/hour and maintained a low velocity of relaxation rate until the end of the test. The

maximum V_R ratio of the steel strand increased from 0.7% to 1.8%, 2.4%, and 2.5%/hour as the temperature decreased from 20°C (68°F) to -40°C, -100°C, and -165°C (-40°F, -148°F, and -265°F), respectively. This might imply that low temperatures accelerate the relaxation rate of the steel strand.

Effect of prestressing force on steel-strand relaxation

The prestressing force-to-ultimate tension capacity ratio F_t/F_u of the steel strands, where F_t and F_u are the prestressing force and ultimate tension capacity of the steel strand, respectively, was used to describe the prestressing levels. Figure 6 plots the effects of the F_t/F_u ratio on the relaxation rate of the prestress R at 20°C, -40°C, -100°C, and -165°C (68°F, -40°F, -148°F, and -265°F), respectively. The figure shows that for steel strand at the same temperature, the

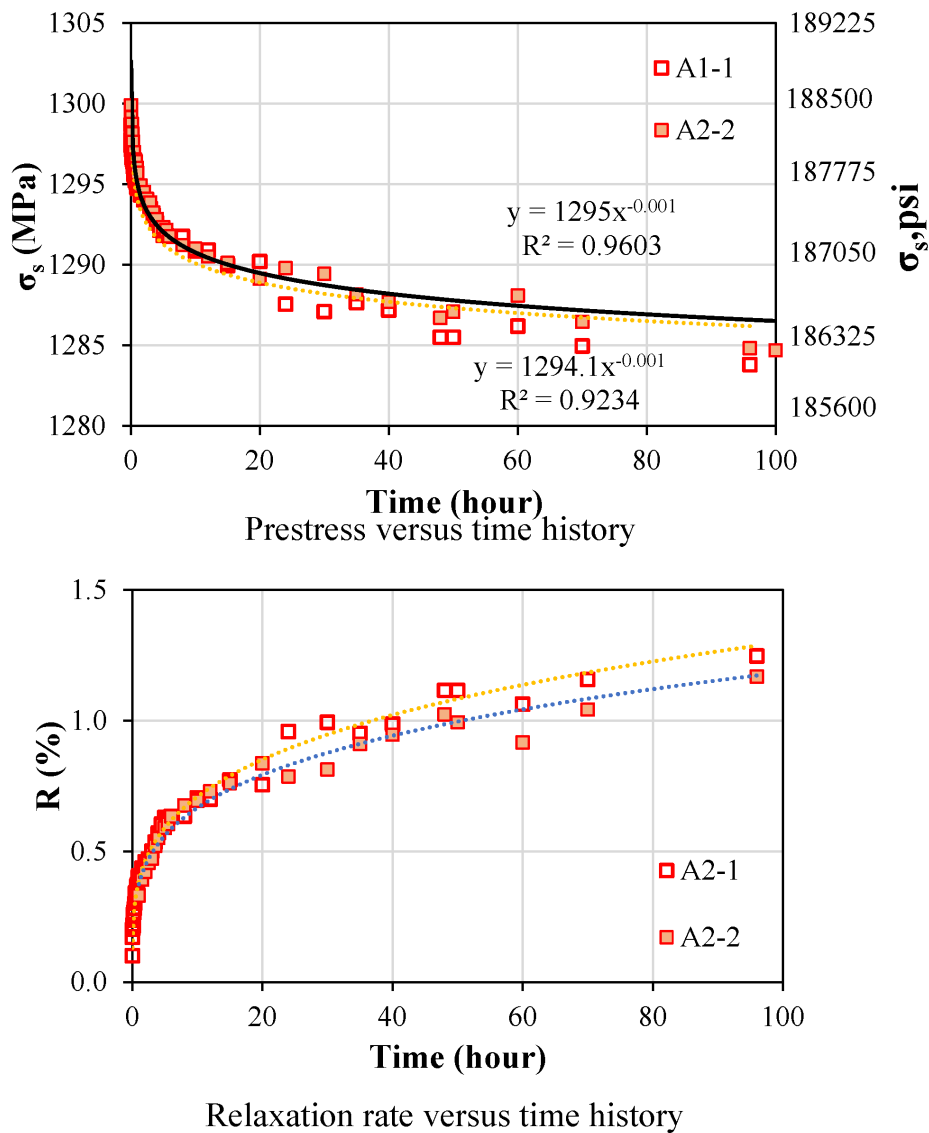
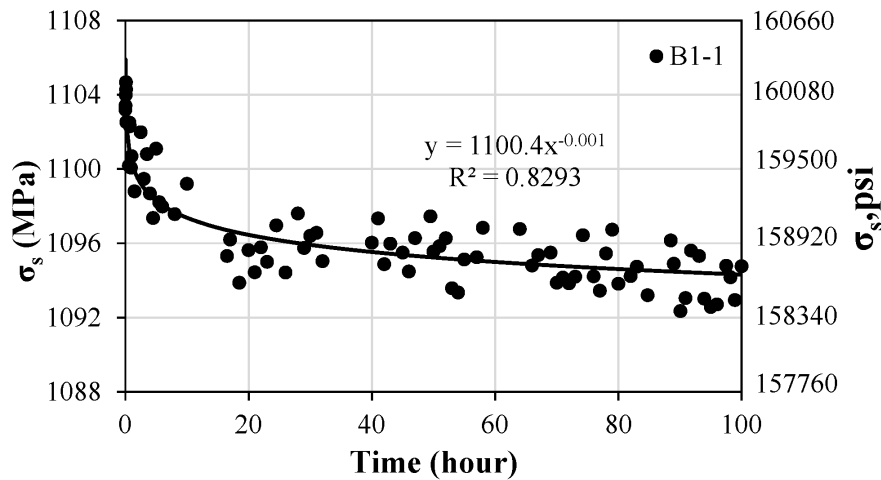


Figure 4. Prestress and relaxation rate curves for specimens A2-1 and A2-2 at ambient temperature of 20°C (68°F). Note: R = relaxation rate of the prestress; R^2 = correlation coefficient; σ_s = prestressing stress.

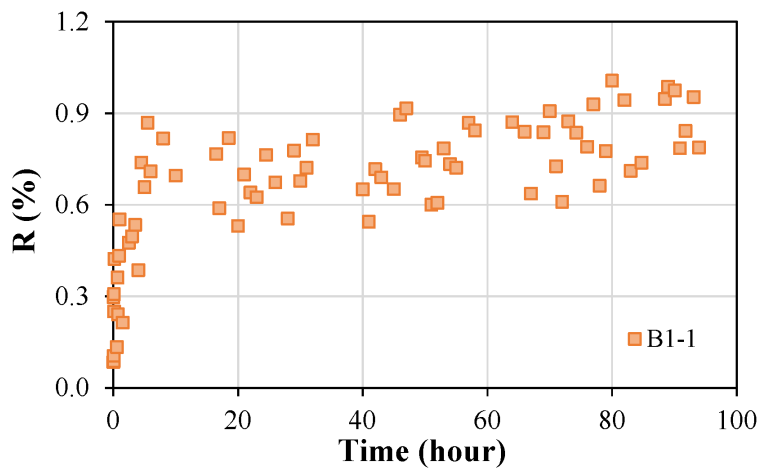
higher the F_t/F_u ratio the greater the effect on the relaxation rate. For example, for specimens A1 to A3 at ambient temperature, as the time increased from 5 to 100 hours, the R ratio for steel strands with a prestressing ratio of $F_t/F_u = 0.75$ increased by 99%, from 0.71% to 1.41%. Meanwhile, the R ratios for steel strands with $F_t/F_u = 0.5$ only increased by 61%, from 0.41% to 0.66%. As the time increased from 5 to 12 hours for the steel strands at temperatures from -40°C to -165°C, the R ratio for steel strands with an F_t/F_u ratio of 0.75 increased slightly faster than for those with an F_t/F_u ratio of 0.65 (Fig. 6). This is because the prestressing force accelerates the flow of the energy in the steel strands, which speeds up the stress relaxation.

Effect of low temperatures on steel-strand relaxation

Figure 8 shows the effects of temperature on steel-strand relaxation under a prestressing ratio of $F_t/F_u = 0.75$ and 0.65. For the steel strands under a prestressing ratio of $F_t/F_u = 0.75$, the relaxation rate of the prestress R first decreased as the temperature decreased from ambient temperature to -40°C (-40°F). However, as the temperature decreased beyond -40°C to -100°C and -165°C (-148°F and -265°F), decreasing the temperature exhibited marginal effects on R . The same observation was found for steel strands under a prestressing ratio of $F_t/F_u = 0.65$. Compared with the effect of the prestressing ratio F_t/F_u , the temperature has less effect on R . Therefore, the time, prestressing ratio, and temperature need to be considered in the analysis of R .



Prestress versus time history



Relaxation rate versus time history

Figure 5. Prestress and relaxation rate curves for specimen B1-1 at low temperature of -40°C (-40°F). Note: R = relaxation rate of the prestress; R^2 = correlation coefficient; σ_s = prestressing stress.

Regression analysis on relaxation rate

The test results showed that time t , prestressing level $P_r = F_i/F_u$, and low temperature T affected the relaxation rate R of the steel strands. The authors therefore developed a mathematical equation to describe the relationship of the R ratio to these three key parameters, t , $P_r = F_i/F_u$, and T . From experimental parametric studies and discussions, the exponential models in this regression analysis were assumed to be the following:

$$R = \alpha t^{\beta} P_r^{\gamma} T^{\eta} \quad (9)$$

where

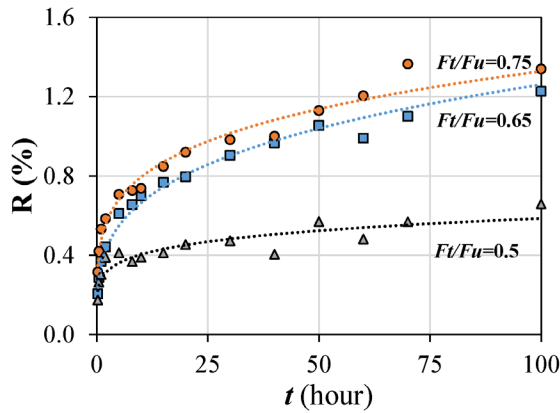
α = constant obtained from the regression analysis

β = constant obtained from the regression analysis

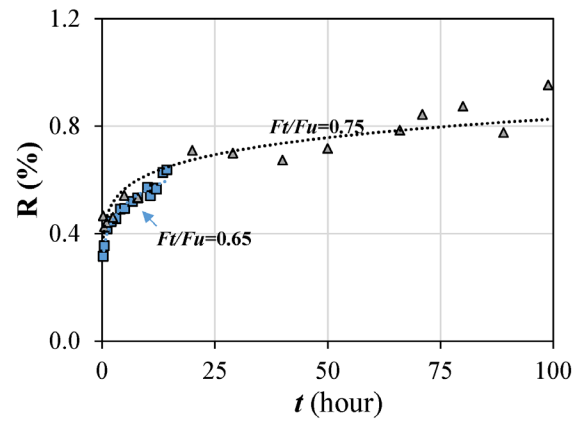
γ = constant obtained from the regression analysis

η = constant obtained from the regression analysis

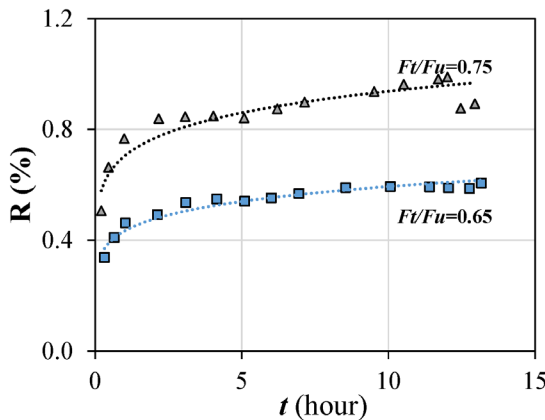
After carrying out the logarithmic transformations to Eq. (9), linear regression analysis was performed. In regression analysis, there are many available methods to select and evaluate the importance of the predictors, such as the backward elimination method, forward elimination method, stepwise regression method, and best subset method. In this paper, the best subset method was used for the regression analysis. In the best subset method, Mallows C_p index, the standard error of the regression S , and the correlation coefficient R^2 , are usually used to evaluate the predicting ability of the regression model.



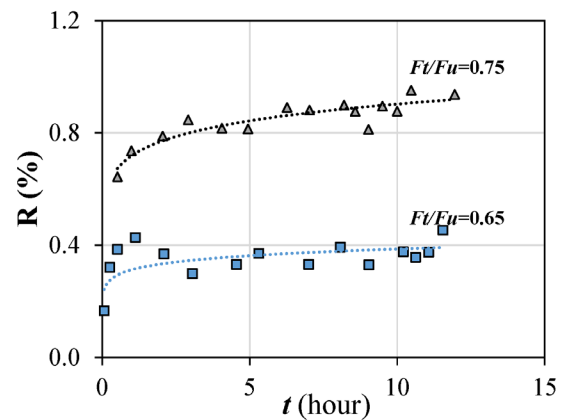
Specimen A1-3 under 20°C



Specimen B1-2 under -40°C



Specimen C1-2 under -100°C



Specimen D1-2 under -165°C

Figure 6. Relaxation rate curves for specimens A1-3, B1-2, C1-2, D1-2. Note: F_t = prestressing force applied to steel strand; F_u = ultimate tensile resistance of steel strand; R = relaxation rate of the prestress. $^{\circ}\text{C} = (^{\circ}\text{F} - 32)/1.8$.

The subset consisting of p predictors from a total of n predictors ($p < n$) offers lower Mallows C_p values (not greater than p) and was the preferred subset.¹⁷⁻²⁰ The correlation coefficient R^2 with a value between 0 and 1.0 indicates how much the test data could be described by the developed regression model. Considering the evaluation criteria, the regression analyses were performed. **Table 6** lists the possible combinations of the three predictors, t , P_r , and T , and the regression results.

The regression analyses show that the model e consisting of three predictors offers the highest correlation ratio of 70.1%, lowest standard error of the regression S of 0.23, and lowest Mallows C_p value of 4.0. This implies that the regression model with three predictors offers the best predictions for the three evaluation criteria.

Equation (10) gives the proposed regression model to predict the relaxation rate of the steel strands with a combination of low temperatures and prestress,

$$R_p = 0.561t^{0.16}P_r^{2.0}T^{0.1} \quad (10)$$

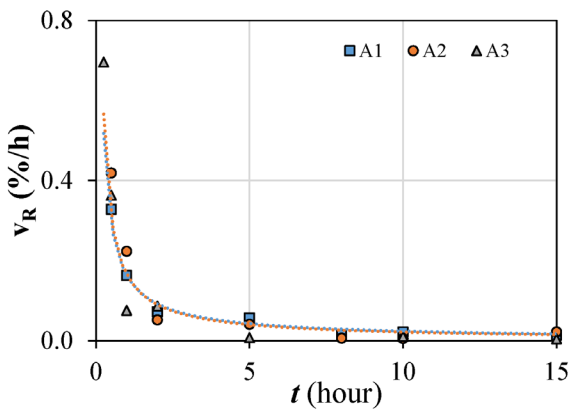
where

R_p = predicted relaxation rate of steel strand at combined low temperature and prestressing stress for temperatures between 108°K and 293°K

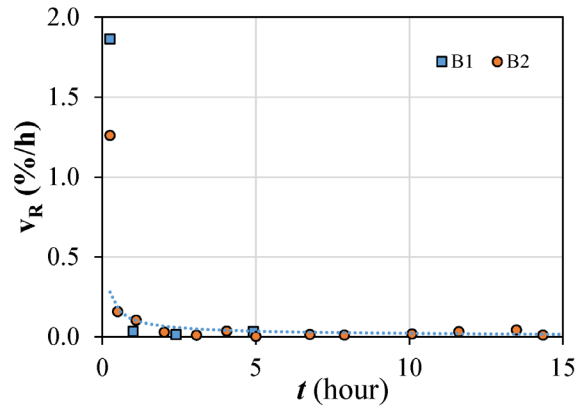
The values of the predicted relaxation rate ratio R_p were compared with the test values R in Tables 2 to 5. The average test-to-prediction ratio for 134 test data points is 1.02 with a coefficient of variation of 0.21. The prediction errors may be caused by the prestressing techniques and the uneven distribution of the temperature in the chamber.

Conclusion

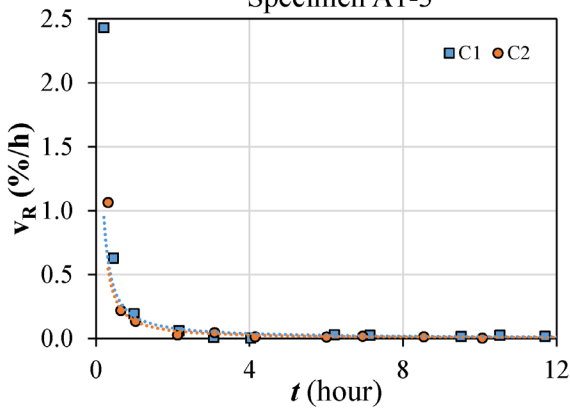
This paper studied the stress relaxation behavior of steel strand experimentally and analytically under different combined prestressing forces ranging from $0.5F_t/F_u$ to $0.75F_t/F_u$ and at low temperatures varying from an ambient temperature of 20°C (68°F) to a low temperature of -165°C (-265°F). The effects of the low temperature and prestressing forces on the



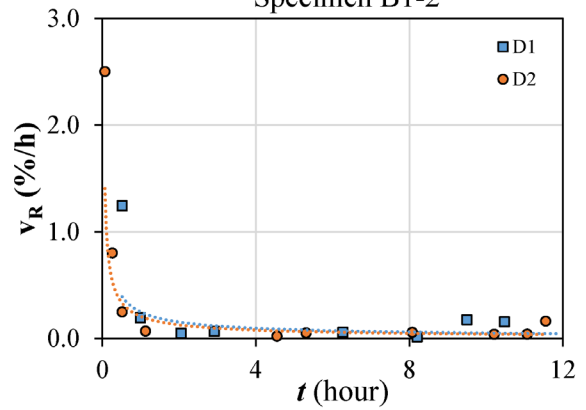
Specimen A1-3



Specimen B1-2

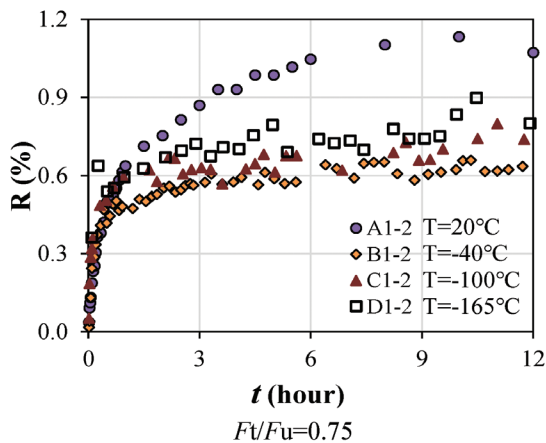


Specimen C1-2

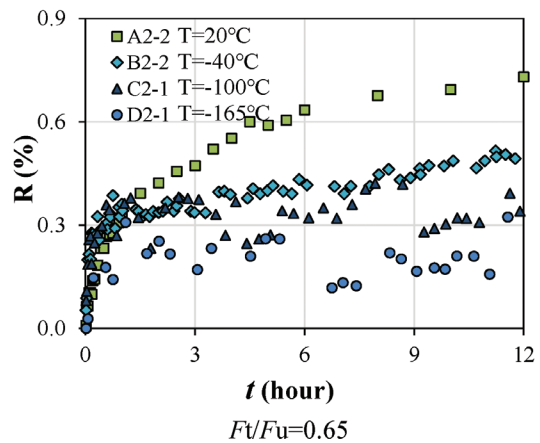


Specimen D1-2

Figure 7. Relaxation rate velocity curves for specimens A1-3, B1-2, C1-2, and D1-2. Note: t = time; V_R = relaxation rate velocity.



$F_t/F_u=0.75$



$F_t/F_u=0.65$

Figure 8. Relaxation rate curves for various specimens. Note: F_t = prestressing force applied to steel strand; F_u = ultimate tensile resistance of steel strand; R = relaxation rate of the prestress; T = temperature.

Table 6. Best subset regression analysis

Model	Response	n	R^2 , %	Mallows C_p	S	$\ln(t)$	$\ln(P_r)$	$\ln(T)$
a	$\ln(R)$	1	35.7	147.5	0.33	✓		
b	$\ln(R)$	1	30.7	168.6	0.34		✓	
c	$\ln(R)$	2	69.2	5.4	0.23	✓	✓	
d	$\ln(R)$	2	36.7	145.2	0.33	✓		✓
e	$\ln(R)$	3	70.1	4.0	0.23	✓	✓	✓

Note: ✓ = considered predictors in the subset regression analysis; n = number of considered predictors; P_r = prestressing levels of steel strand; R = relaxation rate of the prestress; R^2 = correlation coefficient; S = standard error of the regression; t = time; T = temperature.

relaxation behavior of the steel strands were presented and analyzed. A mathematical model was developed based on the regression analysis on the test data to describe the relationship between the relaxation rate and the influencing parameters. Based on these tests and analysis, the following conclusions can be drawn:

- The relaxation rate reduced significantly during the first half hour after prestressing. After five hours, the velocity of the relaxation rate stabilized until the end of the test at 100 hours. The velocity of the relaxation rate during the first half hour increased from 0.7% to 1.8%, 2.4%, and 2.5% per hour as the temperature decreased from 20°C (68°F) to -40°C, -100°C, and -165°C (-40°F, -148°F, and -265°F), respectively.
- The prestressing force-to-ultimate tension capacity ratio F_t/F_u had a positive effect on the relaxation rate. As the time increased from 5 to 100 hours at the same temperature, the relaxation rate of the steel strands with an F_t/F_u ratio of 0.75 increased by 99% compared with 61% for steel strand with an F_t/F_u ratio of 0.5. This observation also applied to the steel strands at low temperatures of -40°C, -100°C, and -165°C (-40°F, -148°F, and -265°F).
- Compared with the relaxation rate of steel strand at ambient temperature, low temperatures tend to slightly reduce the relaxation rate of steel strand under different prestressing levels. However, this effect becomes weak after the temperature decreases beyond -40°C (-40°F) to -100°C and -165°C (-148°F and -265°F). The effect of low temperatures on the relaxation rate is less than that of prestressing levels.
- Based on the regression analysis of the test data by the best subset method, Eq. (10) was developed to predict the relaxation rate of steel strand at low temperatures ranging from 20°C (68°F) to -165°C (-265°F) and prestressing levels from $0.5F_t/F_u$ to $0.75F_t/F_u$. The average test-to-prediction ratio for the 134 test data points was 1.02, with a coefficient of variation of 0.21. Equation (10) may be used to predict the relaxation rate of steel

strand under different prestressing levels as well as at different low temperatures.

The test results and developed regression models were based on limited test data, and these experimental observations and developed models may only be applicable in these particular conditions. Further validation may still be required for design purposes.

Acknowledgments

This work was funded by the National Natural Science Foundation of China (grant 51978459). The authors gratefully express their gratitude for this support. The authors declare that they have no conflict of interest and complied with ethical standards.

References

1. Fernández, R. P., and M. L. Pardo. 2013. "Offshore Concrete Structures." *Ocean Engineering* 58: 304–316.
2. Gautier, D. L., K. J. Bird, R. R. Charpentier, A. Grantz, D. W. Houseknecht, T. R. Klett, T. E. Moore, J. K. Pitman, C. J. Schenk, J. H. Schuenemeyer, K. Sørensen, M. E. Tennyson, Z. C. Valin, and C. J. Wandrey. 2009. "Assessment of Undiscovered Oil and Gas in the Arctic." *Science* 324 (5931): 1175–1179.
3. Yan, J. B., J. Y. R. Liew, M. H. Zhang, and J. Y. Wang. 2014. "Mechanical Properties of Normal Strength Mild Steel and High Strength Steel S690 in Low Temperature Relevant to Arctic Environment." *Materials & Design* 61: 150–159.
4. Stepanova, N. A. 1958. "On the Lowest Temperatures on Earth." *Monthly Weather Review* 86 (1): 6–10.
5. Xie, J., X. Li, and H. Wu. 2014. "Experimental Study on the Axial-Compression Performance of Concrete at Cryogenic Temperatures." *Construction and Building Materials* 72: 380–388.

6. Elices, M., H. Corres, and J. Planas. 1986. "Behaviour at Cryogenic Temperatures of Steel for Concrete Reinforcement." *ACI Journal* 84 (3): 405–411.
7. Lahlou, D., K. Amar, and K. Salah. 2007. "Behavior of the Reinforced Concrete at Cryogenic Temperatures." *Cryogenics* 47 (9): 517–525.
8. Ehlers, S., and E. Østby. 2012. "Increased Crashworthiness Due to Arctic Conditions—The Influence of Sub-zero Temperature." *Marine Structures* 28 (1): 86–100.
9. Planas, J., H. Corres, and M. Elices. 1988. "Behaviour at Cryogenic Temperatures of Tendon Anchorages for Prestressing Concrete." *Materials and Structures* 21 (4): 278–285.
10. Nie, Z. M. 2012. "Experimental Study on Bonding Properties between Steel Wire and Concrete or Cement Slurry at Cryogenic Temperatures." Master's thesis. Tianjin University, China.
11. Liu, J., N. Li, and Z. H. Chen. 2007. "Experiment Study on the Linear Expansion Factor of Cables." *Low Temperature Architecture Technology* 1: 54–55 (in Chinese).
12. Chen, Z. H., and Z. S. Liu. 2010. "Experimental Research of Linear Thermal Expansion Coefficient of Cables." *Journal of Building Materials* 13 (5): 626–631.
13. Dahmani, L., A. Khenane, and S. Kaci. 2007. "Behavior of the Reinforced Concrete at Cryogenic Temperatures." *Cryogenics* 47 (9-10): 517–525.
14. Ministry of Housing and Urban-Rural Development of the People's Republic of China. 2010. *Code for Design of Concrete Structures*. GB 50010-2010. Beijing, China: Standardization Administration of China.
15. China Nonferrous Metals Industry Association. 2013. *Metallic Materials—Tensile Stress Relaxation—Method of Test*. GB/T 10120-2013. Beijing, China: Standardization Administration of China.
16. China Iron and Steel Industry Association. 2008. *Steel for Prestressed Concrete—Test Methods*. GB/T 21839-2008. Beijing, China: Standardization Administration of China.
17. Mallows, C. L. 1995. "More Comments on C_p ." *Technometrics* 37 (4): 362–372.
18. Cohen, J., P. Cohen, S. G. West, and L. S. Aiken. 2003. *Applied Multiple Regression/Correlation Analysis for the Behavioral Sciences*. 3rd ed. Mahwah, NJ: Lawrence Erlbaum Associates Inc.
19. Thompson, M. L. 1978. "Selection of Variables in Multiple Regression: Part I. A Review and Evaluation." *International Statistical Review* 46 (1): 1–19.
20. Mallows, C. L. 1973. "Some Comments on C_p ." *Technometrics* 15 (4): 661–675.

Notation

A_{ps}	= cross-sectional area of steel strand
C_p	= Mallows index
E_s	= Young's modulus of elasticity of steel strand
F_t	= prestressing force applied to steel strand
F_u	= ultimate tensile resistance of steel strand
F_0	= target tension force on steel strand
l	= total length of steel strand
l_1, l_2	= length of steel strand outside cooling chamber
l_3	= length of steel strand in cooling chamber
l_3	= length between holding frame
n	= predictors subset
p	= predictors subset
P_r	= prestressing level
R	= relaxation rate of the prestress
R_p	= predicted relaxation rate
R_{t_1}	= relaxation rate at time t_1
R_{t_2}	= relaxation rate at time t_2
R^2	= correlation coefficient
S	= standard error of regression
t	= time
t_n	= time point
t_0	= time point at zero
T	= temperature

T_n	= testing temperature in chamber at current time t_n	$\Delta\sigma$	= change in stress
$T_{n,l}$	= average value of the temperature at location A (or B) at time t_n	η	= regression analysis constant
$T_{n,r}$	= ambient temperature at time t_n	σ_s	= prestressing stress
T_0	= testing temperature in chamber at time t_0	σ_{s0}	= prestress at initial state
$T_{0,l}$	= average value of the temperature at location A (or B) at time t_0	σ_{st}	= prestress at time t
$T_{0,r}$	= ambient temperature at time t_0		
V_R	= relaxation rate velocity		
X_n	= relative displacement of the strand monitored by the two linear variable displacement transducers installed on the two ends of the strand at time t_n		
X_0	= relative displacement of the strand monitored by the two linear variable displacement transducers installed on the two ends of the strand at time t_0		
α	= regression analysis constant		
α_m	= linear expansion coefficient at temperature		
$\alpha_{m,l}$	= linear expansion coefficient corresponding to $(T_{n,l} + T_{n,r})/2$		
$\alpha_{m,r}$	= linear expansion coefficient corresponding to $(T_{n,r} + T_{n,l})/2$		
α_t	= linear expansion of steel strand		
$\alpha_{t,f}$	= linear expansion coefficient of holding frame		
β	= regression analysis constant		
γ	= regression analysis constant		
ΔF_D	= error force due to strain deformation		
$\Delta F_{0,l}$	= modified prestressing force acting on the steel strand outside the chamber along l_1 (Fig. 3)		
$\Delta F_{0,r}$	= modified prestressing force acting on the steel strand outside the chamber along l_2 (Fig. 3)		
ΔF_1	= modified prestressing force acting on the steel strand due to linear expansion of strand inside the cooling chamber		
ΔT	= change of temperature in steel strand		

About the authors



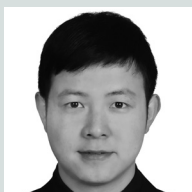
Jia-Bao Yan is an associate professor in the School of Civil Engineering at Tianjin University in Tianjin, China. He received his PhD from National University of Singapore. His research interests

include steel-concrete composite structures, reinforced concrete, and prestressed concrete structures.



Jian Xie is a professor at Tianjin University. He received his PhD in structural engineering from Tianjin University. His research interests include material properties and structural behavior of reinforced concrete and pre-

stressed concrete at cryogenic temperatures, optimization design of liquid natural gas tanks, and retrofitting of buildings in seismic areas.



Kanran Ding is an engineer at Beijing New Airport Construction Headquarters. He received his master's degree in structural engineering from Tianjin University. His research interests include material properties and structural

behavior of reinforced concrete and prestressed concrete at cryogenic temperatures and engineering management.

Abstract

This paper presents the results of experimental and analytical studies on the stress relaxation behavior of steel strand under combined prestressing forces and low temperatures. An 18-specimen test program was conducted to investigate the stress relaxation behavior of steel strand under prestressing forces of 0.5 to 0.75 times the ultimate tension capacity and at temperatures ranging from 20°C (68°F) to -165°C (-265°F). The test results show the relaxation behavior of the steel strands as the time increased from 0 to 100 hours after prestressing and the effects of low temperatures and prestressing levels on the relaxation behavior. Based on the test results and using the best subset regression method, a mathematical model was developed to predict the relationship between the relaxation rate and different influencing parameters, including time, prestressing levels, and low temperature. The accuracy of the regression model was checked through validation against 134 test data points. Finally, a design equation is proposed based on these extensive validations.

Keywords

Liquefied natural gas container, low temperature, material properties, prestressing relaxation, relaxation, steel strand.

Review policy

This paper was reviewed in accordance with the Precast/Prestressed Concrete Institute's peer-review process.

Reader comments

Please address any reader comments to *PCI Journal* editor-in-chief Tom Klemens at tklemens@pci.org or Precast/Prestressed Concrete Institute, c/o *PCI Journal*, 200 W. Adams St., Suite 2100, Chicago, IL 60606. [f](#)